CORROSION INHIBITION OF THE AZ91D MAGNESIUM ALLOY BY N-SALICYLIDENEANILINE SCHIF BASE COMPOUND

D. Seifzadeh, R. Asadpour Joghani

Physical Chemistry Research Laboratory, Applied Chemistry Department, Faculty of Basic Science, University of Mohaghegh Ardabili, Ardabil, Iran

Abstract

The inhibition effect of N-Salicylideneaniline Schiff base against AZ91D alloy corrosion in 0.01 M HCl was examined using potentiodynamic polarization and Electrochemical Impedance Spectroscopy (EIS) methods. The current of both the anodic and cathodic reactions of the corrosion process were decreased while the values of the corrosion potential were not changed significantly indicating that the Schiff base compound acts as mixed–type corrosion inhibitor. EIS measurements were also confirmed the inhibition effect of the Schiff base against AZ91D alloy corrosion. As the inhibitor concentration increased the polarization resistance increased due to more inhibitor adsorption on the surface. Moreover, Scanning Electron Microscopy (SEM), and X–Ray diffraction (XRD) have been used to investigate the corrosion inhibition of the Schiff base compound. SEM images showed that the corrosion damage of the alloy surface reduced in the presence of the Schiff base. The intensity of the characteristic XRD peaks of α phase of the AZ91D alloy was increased in the presence of the Schiff base compound indicating lower corrosion of the alloy sample due to the inhibition effect.

Key words: *magnesium alloy, corrosion inhibition, schiff base, EIS, SEM, XRD*

1. INTRODUCTION

Magnesium alloys are the lightest constructional metallic materials with sufficient hardness and so they are promising candidate for use in different industrial applications especially in automobile industry where any weight reduction leads to reduction in fuel consumption and air pollution. Also, magnesium alloys are suitable materials for application in aerospace, sporting equipment and portable electronic instruments such as mobile phones. Magnesium has also some other advantageous properties such as high thermal conductivity, high dimensional stability, good damping properties, suitable electromagnetic shielding properties and good machinability. Despite the mentioned advantageous, the wider application of the magnesium alloy has limited mostly due to their susceptibility to corrosion which is related with their electrochemical activity (Friedrich and Mordik., 2006). The use of inhibitors is one of the most practical methods for protection of metals against corrosion. The corrosion rate of the magnesium is high due to its electrochemical activity which does not allows for the corrosion inhibitors to adsorb on the surface and therefore, the corrosion inhibition of the magnesium alloys has not fully investigated. However, the corrosion inhibition effect of some chemical compounds including; polyaspartic acid (Yang et al., 2015), 2–Hydroxy–4–methoxy–acetophenone (Hu et al., 2013), 8–hydroxyquinoline (Seifzadeh et al., 2013; Gao et al., 2010), anionic surfactants (Frignani et al., 2012), lactobiono–tallowamide (LTA) (Slavcheva et al., 2005), Stearate (Dindodi and Shetty, 2014), Tetraphenylporphyrin (Hu et al., 2012), and Schiff base compounds (Thirugnanaselvi et al., 2014; Seifzadeh et al., 2013) against the corrosion of magnesium and its alloys has been studied.

Acid pickling is a well–known pre–treatment process to remove impurities from metal surface. Generally, the metallic components have been pickled in hydrochloric acid and sulfuric acid solutions before the final treatments such as electroplating, electroless plating and coating (Ashassi–Sorkhabi et al., 2006; Makhlouf et al., 1996; Nwaogu et al., 2009). Addition of an appropriate acid inhibitor to acidic pickling solutions is necessary to keep the corrosion and destruction of metals under control.

In the present work, the inhibition effect of N-salicylideneaniline Schiff base compound against AZ91D alloy corrosion in 0.01 M HCl solution has been investigated using electrochemical methods

Moreover Scanning Electron Microscopy (SEM) and Energy Dispersive X–Ray Spectroscopy (EDX) methods were used as complementary methods to study the corrosion inhibition effect.

2. EXPERIMENTAL DETAILS

2.1. Materials

The chemical structure of the N-salicylideneaniline Schiff base compound is shown in Fig. 1.

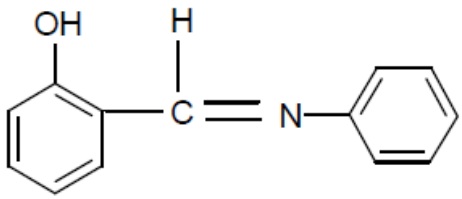


Fig. 1. The chemical structure of the N-salicylideneaniline compound

The Schiff base was synthesized by a condensation reaction between the salicylaldehyde and aniline. First, 10 mL ethanol solution containing 0.018 mol of salicylaldehyde was gradually added to 10 mL ethanol solution containing 0.018 mol of aniline. Then, the mixture was gently stirred for about 3 h and an orange solution was obtained. Finally, the obtained solution was kept in the Refrigerator and the yellow crystals were obtained. The obtained product was purified several times by re-crystallization from ethanol. Fig. 2 shows the FTIR spectrum of the synthesized Schiff base compound. The characteristic peak of the imine group can be observed at 1618 cm^{-1}.

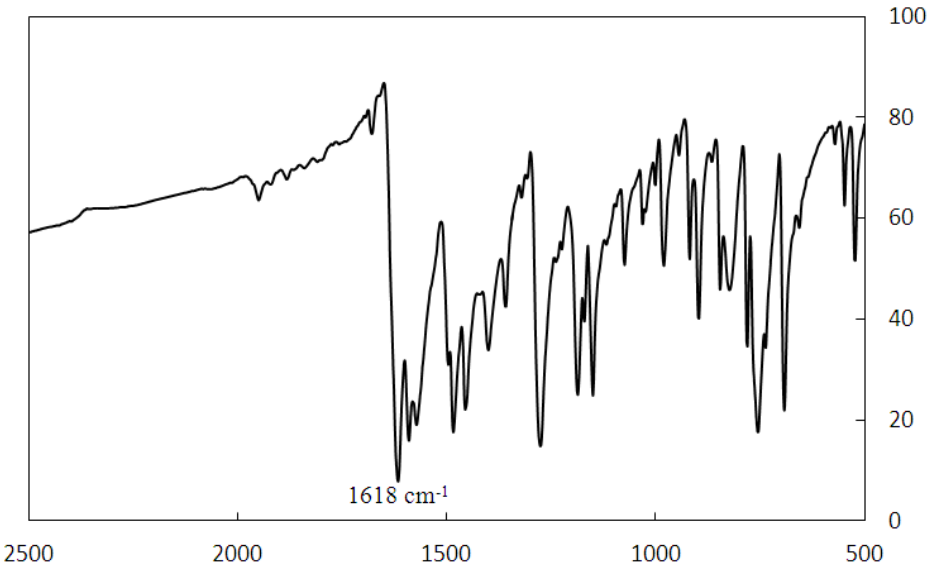


Fig. 2. FTIR spectrum of the synthesized Schiff base compound

AZ91D magnesium alloy samples with a surface area of 1 cm^2 were used as substrate. The acid solutions 0.01 M HCl as corrosive media were made from analytical grade 37% HCl (from Merck). The concentration range of the inhibitor employed was 1×10^{-3} to 6×10^{-3} M. AZ91 samples were mounted in polyester (purchase from TABA chemical company) in such a way that only 1 cm^2 of the

samples was in contact with test solutions. Prior to all measurement, magnesium alloy samples were polished successively with a sequence of emery papers of different grades (400, 800 and 1500 grits). Before the testes, the samples were carefully degreased with ethanol, rinsed with double distilled water and finally dried in compressed air.

2.2. Corrosion tests

Potentiodynamic polarization and EIS tests were carried out using μAUTOLAB3 Potentiostat–Galvanostat. Electrochemical experiments was performed using the three component electrochemica cell consisting of mounted alloy samples as working electrode, platinum sheet as counter electrode and saturated Ag/AgCl electrode as reference electrode. For polarization measurements, the potential was scanned with a scan rate of 1 mVs^{-1} in the cathodic to anodic direction, so that the maximum over voltage was about ±200 mV. EIS measurements were carried out in the frequency range of 1 MHz–10 mHz, at the open circuit potential, by applying 5 mV sine wave ac voltage. To calculate the EIS parameters the Zview2 fitting software was used. All polarization and EIS experiments were performed after 2 h immersion of working electrode in corrosive solution under atmospheric conditions.

2.3. Surface analysis

The surface morphology of the alloy samples after immersion in the blank and inhibited solutions was observed by scanning electron microscopy (LEO, VP 1430), while the chemical composition of the surface was characterized by energy dispersive X-ray spectroscopy (Vega–Tescan). Moreover, the surface structure was studied by the X-ray diffraction (Philips Xpert) method.

3. RESULTS AND DISCUSSIONS

3.1. Potentiodynamic polarization

The potentiodynamic polarization curves of the AZ91D magnesium alloy in the 0.01 M HCl containing different concentrations of the Schiff base compound is given in Fig. 3.

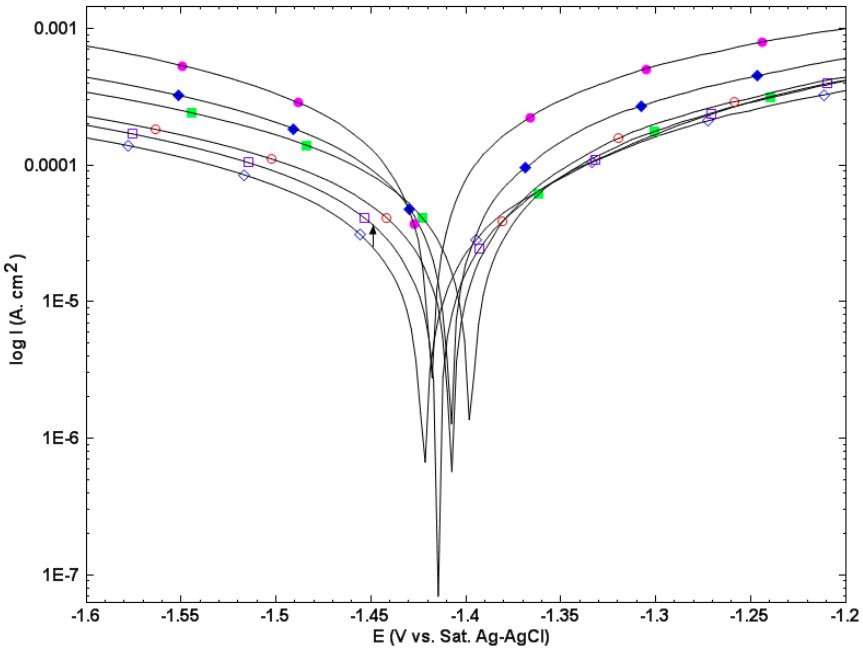


Fig. 3. Polarization curves of the AZ91D magnesium alloy in 0.01 M HCl containing different concentrations of the Schiff base

It is obvious that the current of both the anodic and cathodic branches of the polarization curves were decreased after addition of the Schiff base compound indicating that that the anodic (magnesium dissolution) and cathodic (hydrogen ion reduction) reactions of the corrosion process were inhibited. The inhibition of both the anodic and cathodic reactions was more pronounced with the increasing in the inhibitor concentration. On the other hand, the values of the corrosion potential values did not significantly change meaning that the Schiff base affected both the anodic and cathodic reactions. Moreover, the cathodic and anodic branch of the polarization curves (Fig. 3) giving rise to parallel lines indicates that the Schiff base does not change the values of the Tafel slopes significantly. These results indicated that the Schiff base compound behaves as mixed-type corrosion inhibitor (Ashassi–Sorkhabi et al., 2006; Makhlouf et al., 1996; Nwaogu et al., 2009; Hegazy et al., 2009).

Polarization parameters including; anodic and cathodic Tafel slopes (b_a and b_c respectively), E_{corr} and corrosion current density (j_{corr}) were calculated (Table1). Polarization parameters were obtained by Tafel extrapolation method. Moreover, Table 1 contains values of the percentage inhibition efficiency which were calculated as described elsewhere (Stanly and Parameswaran, 2010).

Table 1. Polarization parameters for AZ91D magnesium alloy in the 0.01 M HCl solution at the absence and presence of the Schiff base at different concentrations

Con.(M)	E_{corr})V vs. Sat. Ag/AgCl(	b_a (mV/dec)	b_c)mV/dec(	j_{corr} (μA. cm^{-2})	%IE
blank	-1.417	160	172	112.7	-
0.002	-1.400	154	167	74.6	33.81
0.003	-1.399	147	166	68.7	39.04
0.004	-1.407	163	127	31.7	71.87
0.005	-1.414	119	161	24.9	77.91
0.006	-1.421	134	167	23.8	78.88

The corrosion current density obtained for the alloy samples tested in the inhibited solutions was lower than the blank solution. The lowest j_{corr} value was observed for 0.006 M inhibitor solution which showed a maximum percentage inhibition efficiency of 78.88 %. The observed corrosion inhibition effect implies that the rate of the corrosion reactions was reduced due to the formation of the inhibitor film over the alloy surface (Ashassi–Sorkhabi et al., 2006; Solmaz, 2010).

3.2. Electrochemical impedance spectroscopy

Electrochemical impedance spectroscopy was also employed as a powerful complementary technique to study the corrosion inhibition effect of the Schiff base in 0.01 M HCl solution. The results of the EIS experiments in the Nyquist plot form were presented in Fig. 4 in the absence (a) and presence (b) of the Schiff base compound. The Nyquist plots for the blank solution (Fig. 4.a) show three well-defined capacitive loops followed by a scattered inductive loop.

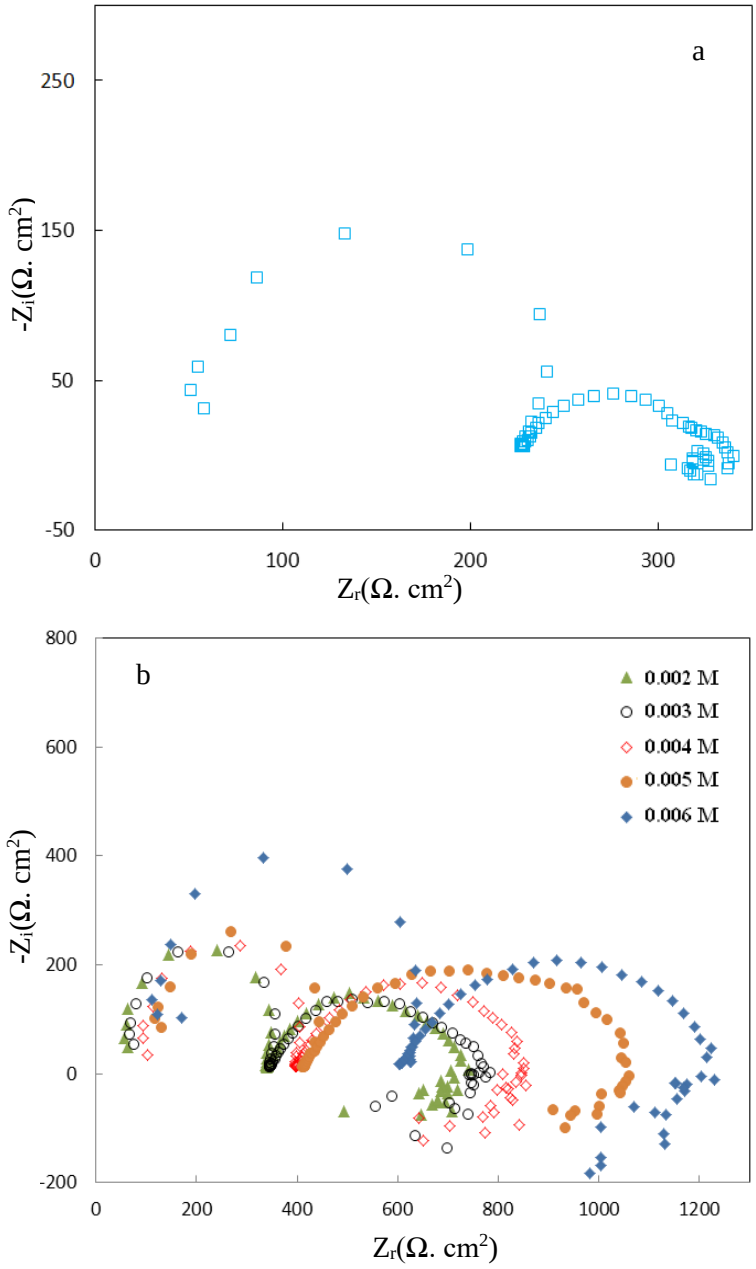


Fig. 4. Nyquist plots of the AZ91D magnesium alloy in 0.01 M HCl in the absence (a) and presence (b) of the Schiff base at different concentrations

The first capacitive loop at the highest frequencies is produced due to adsorption of hydrogen ions while the second one is always related to the charge transfer resistance (R_t) and the double layer capacitance of the magnesium surface. The third capacitive loop is related with the concentration of the univalent magnesium ion in the film free area of the surface. Finally, the inductive loop at lowest frequencies is attributed mainly to the partially protective surface film (Seifzadeh et al., 2013; Song et al., 1997; Cao, 1990).

Appropriate equivalent circuit (Fig. 5a) was used to fitting the EIS data. In this model, R_s, R_t and $R_{(film)}$ characterize the solution resistance, charge transfer resistance and partially protective film resistance respectively while the $R_{(ad)}$ is inserted to account the resistance related with the first capacitive loop at highest frequencies. Also, $CPE_{(dl)}$ and $CPE_{(film)}$ were used to model the capacitive behavior of the

electrical double layer and partially protective film respectively. Moreover, the constant phase element $CPE_{(ad)}$ was added to account for the capacitance of the first loop at highest frequencies. In the used circuit, the constant phase elements (CPE) are used instead of the ideal capacitors due to non-ideal behavior of the electrochemical capacitors.

For the highest concentration of the inhibitor, the second and third capacitive loops merge into a single depressed semicircle (Fig. 4.b) and therefore, a different equivalent circuit consisting only two times constant (Fig. 5.b) was used in fitting process.

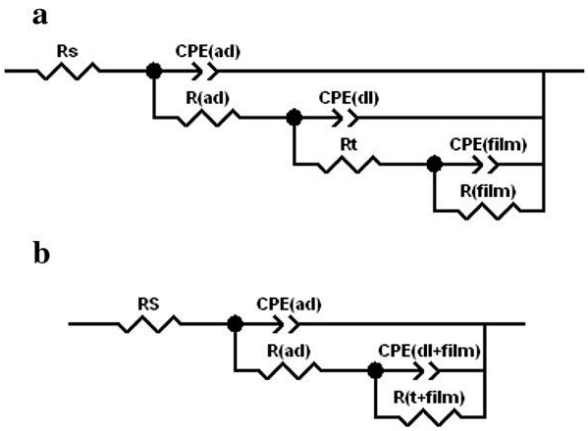


Fig. 5. Equivalent circuit models for the blank (a) and inhibited (b) solutions

The calculated parameters are collected in Table 2. It should be mentioned that the inductive loop elements were not entered in the circuits because the corresponding data were very scattered. Therefore, the relevant data with low frequencies were not taken into account in the fitting process. The fitting was carried out using Zview2 software and the produced data are displayed in Table 2. In this Table, the values of the percentage inhibition efficiency were calculated using the total or (or polarization) resistance as described elsewhere (Seifzadeh et al., 2013). As can be seen, the total resistance of the magnesium surface significantly increases after the addition of the Schiff base of different concentrations, implying that the Schiff base compound used acts as effective corrosion inhibitor for magnesium in the studied corrosive solution. Also as the inhibitor concentration increases the inhibition efficiencies increase probably due to more inhibitor molecules adsorbed on the magnesium surface.

Table 2. Impedance parameters for the AZ91D magnesium alloy in the 0.01 M HCl solution in the absence and presence of the Schiff base inhibitor

Con (M)	Blank	0.002	0.003	0.004	0.005	0.006
CPE_{ad} ($nf.cm^2$)	0.028	0.039	0.0031	0.034	0.0018	0.003
R_{ad} ($\Omega.cm^2$)	150.9	264.5	256.0	275.6	287.2	453.3
CPE_{dl} ($\mu f.cm^2$)	24.4	24.7	36.5	23.7	54.2	35.6
R_t ($\Omega.cm^2$)	123.7	346.1	420.4	444.9	723.7	653.9
CPE_{film} ($mF.cm^2$)	0.40	-	-	-	-	-
R_{film} ($\Omega.cm^2$)	10.2	-	-	-	-	-
R_{total} ($\Omega.cm^2$)	284.8	610.6	676.4	720.5	1010.9	1107.2
%IE	-	53.36	57.89	60.47	71.83	74.28

3.3. Surface analysis

The effect of the inhibitor on the corrosion process of the magnesium alloy was also examined by the SEM images. Fig. 6.a shows SEM image of the magnesium alloy substrate after immersion in 0.01 M HCl solution for 2 h. The micrograph reveals that, the surface was damaged strongly due to the metal dissolution in aggressive solution in the absence of the inhibitor. Fig.6.b shows the image of the magnesium surface after 2 h immersion in 0.01 M HCl solution containing 0.006 M inhibitor. The damage of the metal surface has diminished in the presence of the inhibitor. This may be due to adsorption of the Schiff base compound on the metal surface which is responsible for the corrosion inhibition. In fact, the inhibitor molecule reduces the corrosion rate of the substrate by adsorption on the active corrosion sites.

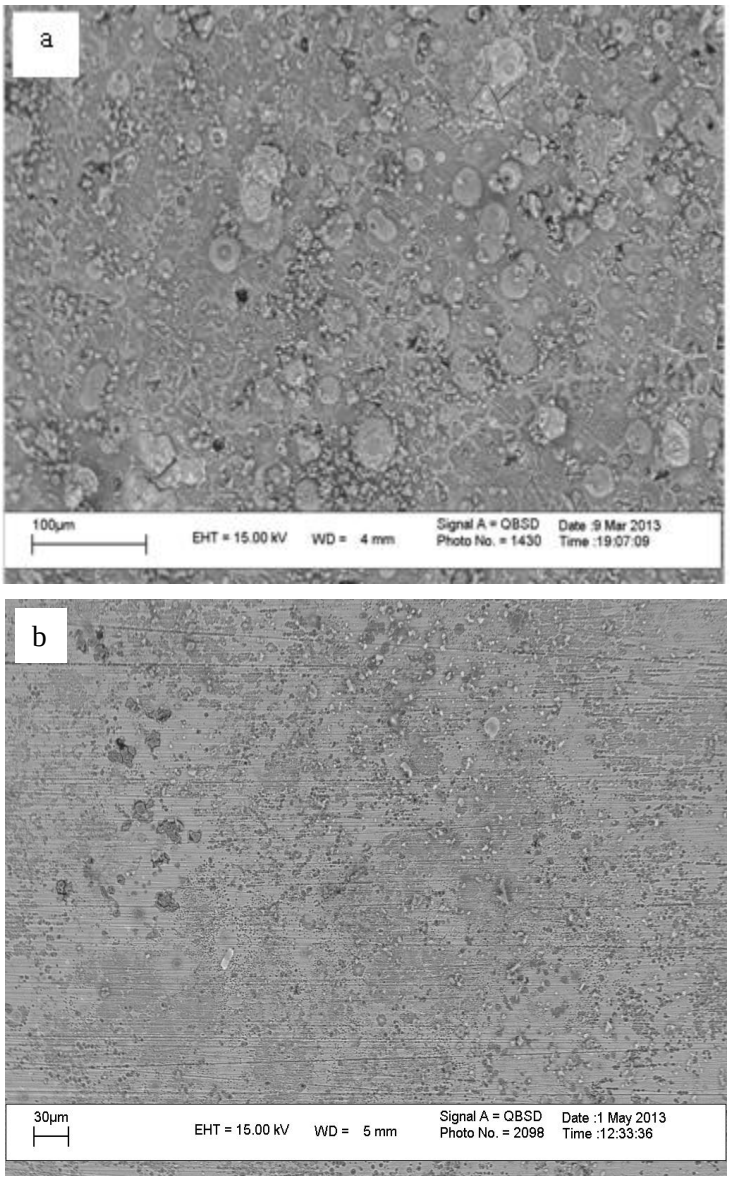


Fig. 6. SEM images of the alloy sample after 2 h immersion in 0.01 M HCl in the absence (a) and presence (b) of the Schiff base inhibitor

Fig. 7 presents the XRD spectrums of magnesium alloy AZ91D after 10 h immersion in the blank (a) and the solution containing 0.006 M of the Schiff base (b). The peaks of α–Mg and β–phase

($Mg_{17}Al_{12}$) of the AZ91D alloy are characterized. It is well–known that the α–Mg phase is more active than the β–phase and is more susceptible to corrosion in the acid solution. The intensity of the peaks corresponding to α–Mg phase increases in the presence of the Schiff base indicating lower corrosion of mg–rich α–Mg phase. Meanwhile, there are some additional peaks at the XRD pattern of the samples immersed in the blank solution which are related to Mg $(OH)_2$ as the corrosion product, but there are no corresponding peaks at the presence of the Schiff base. These facts clearly show the corrosion inhibition performance of the synthesized Schiff base (Zeng et al., 2010; Zhang et al., 2007; Wang et al., 2010).

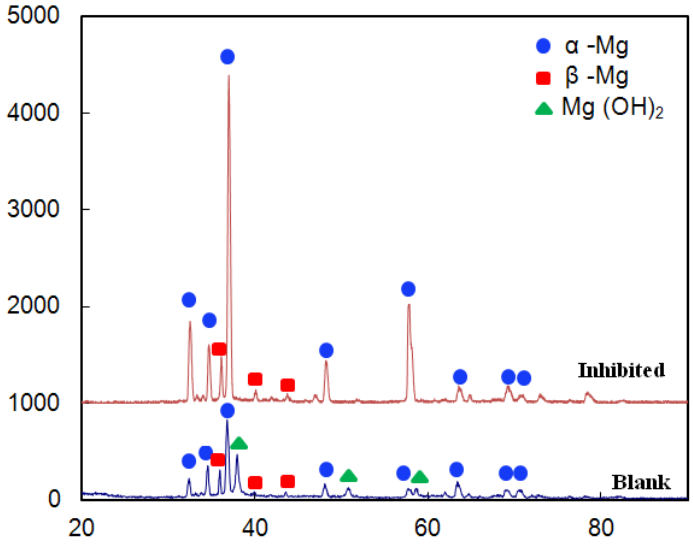


Fig. 7. XRD pattern of the AZ91D alloy after 10 h immersion in the 0.01 M HCl with and without addition of the inhibitor

4. CONCLUSION

1) The *N-Salicylideneaniline Schiff base* is an effective mixed type inhibitor for corrosion of AZ91D alloy in 0.01 M HCl, and its inhibition efficiency increases with increasing the inhibitor concentration.
2) EIS results showed that the total resistance of the alloy surface significantly increases by addition of the Schiff base implying that the Schiff base compound acts as effective corrosion inhibitor for AZ91D alloy in 0.01 M HCl.
3) SEM images show that the alloy surface was completely damaged due to strong corrosion attack in the blank solution; while the alloy surface is uniform without obvious corrosion defects in the presence of the N-Salicylideneaniline.
4) The intensity of the XRD peaks corresponding to *α*-Mg phase is higher for the sample immersed in the inhibitor containing solution in comparison with the sample immersed in the blank solution, indicating lower corrosion of the alloy surface.

REFERENCES

Ashassi–Sorkhabi, H, Shabani, B, Aligholipour, B & Seifzadeh, D 2006, 'The effect of some Schiff bases on the corrosion of aluminum in hydrochloric acid solution', *Applied Surface Science*, vol. 252, pp. 4039-4047.

Cao, CN, 1990, **'**On the impedance plane displays for irreversible electrode reactions based on the stability conditions of the steady-state—I. One state variable besides electrode potential', *Electrochimica Acta*, vol. 35, pp. 831-836.

Cao, CN 1990, Electrochim. Acta, **'**On the impedance plane displays for irreversible electrode reactions based on the stability conditions of the steady-state—II. Two state variables besides electrode potential**',** *Electrochimica Acta*, vol. 35, pp. 837-844.

Dindodi, N & A. Shetty, N 2014, 2014, 'Stearate as a green corrosion inhibitor of magnesium alloy ZE41 in sulfate medium', *Arabian Journal of Chemistry*, Doi:10.1016/j.arabjc.2012.02.018

Friedrich, H E & Mordik, B L (eds) 2006, *'Magnesium Technology: Metallurgy, Design Data', Applications*, Springer-Verlag, Berlin.

Frignani, A, Grassi, V, Zanotto, F & Zucchi, F 2012, 'Inhibition of AZ31 Mg alloy corrosion by anionic surfactants', *Corrosion Science*, vol. 63. Pp. 29-39.

Gao, H, Li, Q, Dai, Y, Luo, F & Zhang, HX 2010, 'High efficiency corrosion inhibitor 8–hydroxyquinoline and its synergistic effect with sodium dodecylbenzenesulphonate on AZ91D magnesium alloy', *Corrosion Science*, vol. 52, pp. 1603–1609.

Hegazy, MA, 2009, 'A novel Schiff base-based cationic gemini surfactants: Synthesis and effect on corrosion inhibition of carbon steel in hydrochloric acid solution', Corrosion Science, vol. 51, pp. 2610–2618.

Hu, J, Huang, D, Zhang, G, Song, GL & Guo, X 2012, 'A Study on Tetraphenylporphyrin as a Corrosion Inhibitor for Pure Magnesium', *Electrochemical and Solid-State Letters*, vol. 15, 6, pp. C13-C15

Hu, J, Zeng, D, Zhang, Z, Shi, T, Song, GL & Guo, X 2013, '2–Hydroxy–4–methoxy–acetophenone as an environment–friendly corrosion inhibitor for AZ91D magnesium alloy', *Corrosion Science*, vol. 74, pp. 35-43.

Makhlouf, MT, El–Shatory, SA & El–Said, A 1996, 'The synergistic effect of halide ions and some selected thiols as a combined corrosion inhibitor for pickling of mild steel in sulphuric acid solution', *Materials Chemistry and Physics*, vol. 43, pp. 76-82.

Nwaogu, UC, Blawert, C, Scharnagl, N, Dietzel, W& Kainer, KU 2009, 'Influence of inorganic acid pickling on the corrosion resistance of magnesium alloy AZ31 sheet', *Corrosion Science*, vol. 51, pp. 2544-2556.

Seifzadeh, D, Basharnavaz, H & Bezaatpour, A 2013, 'A Schiff base compound as effective corrosion inhibitor for magnesium in acidic media', *Materials Chemistry and Physics*, vol. 138, pp. 794-802.

Seifzadeh, D, Hamzedoust–Hasankiadeh, S & Shamkhali, AN 2013, 'Electrochemical and DFT Studies of 8–hydroxyquinoline as corrosion inhibitor for AZ61 magnesium alloy in acidic media', *Protection of Metals and Physical Chemistry of Surfaces*, vol. 49, pp. 229-239.

Slavcheva, E, Petkova, G & Andreev, P 2005, 'Inhibition of corrosion of AZ91 magnesium alloy in ethylene glycol solution in presence of chloride anions', *Materials Corrosion*, vol. 56, pp. 83-87.

Solmaz, R 2010, 'Investigation of the inhibition effect of 5-((E)-4-phenylbuta-1,3-dienylideneamino)-1,3,4-thiadiazole-2-thiol Schiff base on mild steel corrosion in hydrochloric acid', *Corrosion Science*, vol. 52, pp. 3321–3330.

Song, G, Atrens, A, John, DS, Wu, X & Nairn, J 1997, **'**The anodic dissolution of magnesium in chloride and sulphate solutions', *Corrosion Science*, vol. 39 pp. 1981-2004.

Stanly, J K & Parameswaran, G 2010, 'Corrosion inhibition of mild steel in hydrochloric acid solution by Schiff base furoin thiosemicarbazone', *Corrosion Science*, vol. 52, pp. 224–228.

Thirugnanaselvi, S, Kuttirani, S & Emelda, A R 2014, 'Effect of Schiff base as corrosion inhibitor on AZ31 magnesium alloy in hydrochloric acid solution', *Transactions of Nonferrous Metals Society of China*, vol. 24, pp. 1969-1977.

Wang, L, Zhang, B P & Shinohara, T 2010, 'Corrosion behavior of AZ91 magnesium alloy in dilute NaCl solutions', *Materials and Design*, vol. 31, 857–863.

Yang, L, Li, Y, Qian, B & Hou, B 2015 'Polyaspartic acid as a corrosion inhibitor for WE43 magnesium alloy', *Journal of Magnesium and Alloys* , vol. 3, pp. 47-51.

Zeng, L, Yang, S, Zhang, W, Guo, Y & Yan, C 2010, 'Preparation and characterization of a double–layer coating on magnesium alloy AZ91D', *Electrochimica Acta*, vol. 55, pp. 3376–

3383.

Zhang, W X, He, J G, Jiang, Z H, Jiang, Q & Lian, J S, 2007, 'Electroless Ni–P layer with a chromium–free pretreatment on AZ91D magnesium alloy', *Surface and Coatings Technology*, vol. 201, pp. 4594–4600.